

# Effects Of Some Operating Parameters On Photocatalytic Activity Of Ag–N Co-Doped TiO<sub>2</sub> Nanocomposite Under Visible Irradiation

Gebretinsae Yeabyo Nigussie, Abi Tadesse Mengesha, Desta Gebremedhin Gebrehiwet

Chemistry Department, Mekelle University, Mekelle, Ethiopia;  
Chemistry Department, Haramaya University, Harar, Ethiopia;  
Chemistry Department, Mekelle University, Mekelle, Ethiopia.  
Email: g.tinsae21@gmail.com

**ABSTRACT:** Ag-N/TiO<sub>2</sub> nanoparticles have been prepared from commercial TiO<sub>2</sub> (Degussa P-25). The prepared sample was calcined at 400 °C for 4 hours. The composite was characterized by X-ray diffraction (XRD) analysis was carried out to determine the crystalline phases of the synthesized material, Transmission Electron Microscopy (TEM) used to analyze the size and morphology of nonmaterial, Ultraviolet – Visible Spectroscopy (UV-VIS) to determine the maximum wavelength. The effect of calcination temperature, catalyst loading, initial pH and silver doping on the photocatalytic efficiency of the sample was tested using methyl orange (MO) as a target pollutant. Results shows titanate phase could transform to anatase phase at the calcination temperature higher than 300 °C and with further increase in the calcination temperature from 700 to 900 °C, the intensity of rutile phase increased. TEM images of Ag-N/TiO<sub>2</sub> nanocomposite were measured and the size of the particles is in the range 10–15 nm. While the absorption edge of the nano-composite was observed at an absorption band of 540 nm. Silver content has an optimum value of 0.5 M for achieving high photocatalytic activity. However, too much silver loading will result in a negative effect and photocatalytic degradation of MO decreases. Ag-N/TiO<sub>2</sub>- visible photocatalysts achieved the highest photodegradation efficiency with a MO conversion of 87.42% and 84.32% after 180 min of visible and UV irradiation respectively. The effects of pH on the photodegradation efficiency, which include optimum amount of Ag-N/TiO<sub>2</sub> (400 mg/L) photocatalyst and fixed concentration of MO (100 ppm) the highest degradation was observed at pH 2.

**Key words:** as-synthesized photocatalyst, photodegradation, Methyl orange, Ag-N/TiO<sub>2</sub>

## 1. INTRODUCTION

Oxide semiconductor photocatalysis has attracted extensive attention due to its wide potential application in environmental protection procedures such as air purification, water disinfection, hazardous waste remediation, and water purification [1]. Among various oxides semiconductor photocatalysts titanium dioxide has been intensively investigated as a photocatalyst and is still the most efficient, most practical, and most studied photocatalyst despite extensive efforts to find photocatalytic materials out performing TiO<sub>2</sub>. The photocatalytic reactions on TiO<sub>2</sub> are initiated by absorbing UV photons that can excite valence band (VB) electrons to conduction band (CB) in the solid lattice and are completed through the subsequent interfacial electron transfers and thermal reactions occurring on the surface [1, 2]. However, because of the wide band gap of titanium dioxide (3.2 eV), its practical application is inhibited for the low photon utilization efficiency and need of an ultraviolet excitation source which accounts for only small fraction of the solar light (3-5%) [3]. Therefore, it is an important and challenging issue to develop new TiO<sub>2</sub> photocatalytic system with enhanced activities under both UV and visible light irradiation compared with the bare TiO<sub>2</sub>, improving the utilization efficiency of the solar energy. In order to utilize TiO<sub>2</sub> as a photocatalyst with combination of both UV and visible, different factors such as preparation method, modification method, and operational parameters such as concentration of the catalyst (TiO<sub>2</sub>), calcination temperature, pH of the system, concentration of pollutants, nature of the precursor, irradiation time, intensity of radiation, nature of the photocatalyst should be taken in to account [4, 5, 6, 7]. Ionic dyes discharged from the textile, printing, and tanning industries commonly are toxic, and some are carcinogenic and mutagenic, causing deterioration in water quality, influencing the photosynthetic activity of aquatic organism [8]. The main aim of this study was effect of operating parameters on photocatalytic activity of Ag loaded N-

doped TiO<sub>2</sub> for degradation of methyl orange dye. The as-synthesized semiconductor nanomaterial has been used to investigate the effects of pH, catalyst load, calcination temperature and dopant content.

## 2. EXPERIMENTAL

### 2.1 Materials

TiO<sub>2</sub> (Degussa p-25, Germany), Urea (BLULUX), Methyl Orange (MW 327.33, Berckland Scientific Supplies), Ammonium Hydroxide (Abron Chemicals) and Silver Nitrate (MW 169.87, BULUX),. All chemicals were of analytical grade and used as received.

### 2.2 Methods

Preparation of N-doped TiO<sub>2</sub>- 10 gm of TiO<sub>2</sub> and 30 gm of urea were mixed well with predetermined TiO<sub>2</sub>/urea molecular ratio (1:3) for a few minutes in agar mortar. Then the mixture was transferred in a ceramic crucible and calcined at 400 °C for four hours and then cooled. Preparation of Ag loaded N-doped TiO<sub>2</sub> – A 10 gm of the as-synthesized N-doped TiO<sub>2</sub> from the above was mixed with 10 ml of 0.2018 M AgNO<sub>3</sub> aqueous solution in a crucible. The liquid was dried at 110 °C for 30 minutes in an oven and the dried powder was calcined in a furnace at 400 °C for 4 hours. The obtained powder was characterized and used for photocatalytic studies. Again the prepared Ag-N-doped TiO<sub>2</sub> was then calcined at 100, 200, 300, 400, 500, 600, 700, 800, 900 and 1,000 °C in air for 2 h to show the effect of temperature.

### 2.3 Characterization Methods

For determining the type, phase state and crystallite size of the as-synthesized photocatalysts, X-ray diffraction (XRD) patterns were obtained on BRUKER D8 XRD, AXS GmbH, Karlsruhe, West Germany using a Cu target K $\alpha$  radi-

tion ( $\lambda = 1.5405\text{\AA}$ ) at GSE. The shape and size of nanocomposite were obtained from transmission electron microscopy (TEM) with model TEM, JEOL 3010 (I.I.T. Chennai). For determining absorption edge and the band gap energy (E<sub>bg</sub>) of the synthesized photo-catalyst, their diffuse absorption spectra were obtained using UV-Visible spectrophotometer (Perkin Elmer: model Lambda 950) over the wavelength range of 200–800 nm.

**2.4 Photocatalytic degradation study using different concentrations of silver**

10 g of the as-synthesized N-doped TiO<sub>2</sub> was mixed with 10 ml of 0.1 M, 0.2018 M, 0.25 M, 0.5 M, 0.75 M and 1 M of silver aqueous solution in a crucible. The liquid was dried at 110 °C for 30 minutes in an oven and the dried powder was calcined in a furnace at 400 °C for 4 hours. The obtained powder was taken to photocatalytic degradation. The experiment was carried out by varying the above concentrations by keeping the others parameters constant.

**2.5 Photocatalytic degradation study using different pH range**

To evaluate the effect of pH on the photocatalytic activity of Ag-N/TiO<sub>2</sub> photocatalyst for the degradation of methyl orange under UV/visible irradiation was studied. The experiment was carried in the pH range of (2-9). The pH of the solution was adjusted by using H<sub>2</sub>SO<sub>4</sub> and NaOH. A 0.5 g of Ag-N/TiO<sub>2</sub> nanoparticles was immersed into 250 ml of dye solution by stirring and continuously air was bubbled. A blank solution was prepared by the same method without Ag-N/TiO<sub>2</sub> sheet. At regular intervals of 20 minute, 10 ml of MO solution was sampled and its concentration measured by its absorbance at 510 nm using UV – Visible spectrophotometer.

**3. RESULTS AND DISCUSSIONS**

**3.1 XRD**

The crystalline phase and particle size of Ag-N/TiO<sub>2</sub> nanoparticles were analyzed by X-ray diffraction (XRD) measurements which were carried out at room temperature by using Siemens X-ray diffractometer [BRUKER D8 XRD, AXS GmbH, Karlsruhe, West Germany using a Cu K $\alpha$  radiation ( $\lambda = 0.15406$  nm)]. The average crystallite size of the as-synthesized photocatalysts can be calculated using the Debye-Scherrer formula, as used by [9].

$$D = \frac{0.9\lambda}{\beta \cos\theta} \tag{1}$$

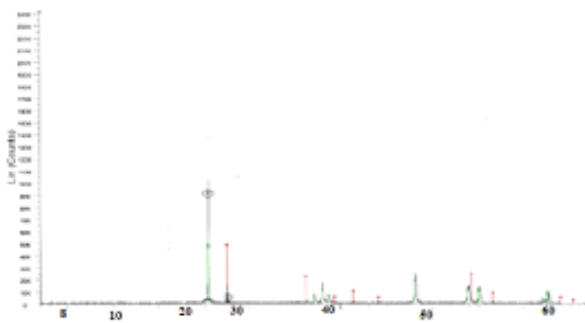


Fig. 1. XRD Spectra of Ag - N co-doped TiO<sub>2</sub>

The crystallographic characteristic of the films was examined using X-ray diffraction shown in (Fig. 1). In this case 2 $\theta$  range from 8 to 660, five peaks were observed: 25.413, 38.5, 48.0, 53.5 and 62.50 for the anatase film and seven peaks at 27.539, 36.1, 39.2, 41.4, 44.0, 54.4 and 56.70 were observed for the rutile film. Strong peak was observed for both anatase and rutile at 2 $\theta$  = 25.4130 and 27.5390 respectively (Fig. 1). TiO<sub>2</sub> crystallite size of anatase and rutile can be estimated as 41.51 and 66.98 nm by the Scherrer equation respectively (Table 1). It is noticed that no XRD peaks corresponding to Ag additions can be revealed. This may be attributed to the well dispersion of nanocrystalline Ag particles in the TiO<sub>2</sub> matrix, the overlapping of Ag XRD peak or silver oxide particles are not crystallized on TiO<sub>2</sub> surface. There are diffraction peaks at (2 $\theta$ ) 27.4, 36.1, 39.2, 41.2, 44.0, 54.4, and 56.7° can be indexed to the (110), (101), (200), (111), (210), (211), and (220) crystal planes of rutile TiO<sub>2</sub> [10]. The diffractogram of the anatase film shows peaks at 25.4° and 37.7°, due to diffraction from the (101) and (004) planes of anatase [11].

**Table 1.** Average crystal size (D) of the as-synthesized photocatalyst

| Sample           | 2 $\theta$ (Degree) | $\beta$ (Radian) | D (nm) |
|------------------|---------------------|------------------|--------|
| ANT <sub>R</sub> | 27.539              | 0.00213          | 66.98  |
| ANT <sub>A</sub> | 25.413              | 0.0034           | 41.51  |

From the data obtained we can see that in case of rutile significant increase in crystallite size was observed. We obtained the results similar to other studies [12]. Concerning the effect of crystallite size of both anatase and rutile phases on the photoactivity. These models suggest that rutile can grow to a size larger than anatase due to sintering and growth of nanophase titania [13].

**3.2 Effect of Calcination Temperature**

The XRD technique was used to investigate the phase transformation of the prepared samples. Fig. 2 shows the XRD patterns of the prepared samples with out and with calcination at 100, 200, 300, 400, 500, 600, 700, 800, 900 and 1000 °C in air for 2 h. Titanate phase could transform to anatase phase at the calcination temperature higher than 300 °C. With increasing calcination temperature from 300 to 800 °C, the peak intensities of anatase increased, indicating the improvement of crystallization of anatase phase. With further increase in the calcination temperature from 700 to 900 °C, the intensity of rutile phase increased. When the calcinations temperature reached 1000 °C, only rutile phase was found in the XRD pattern.

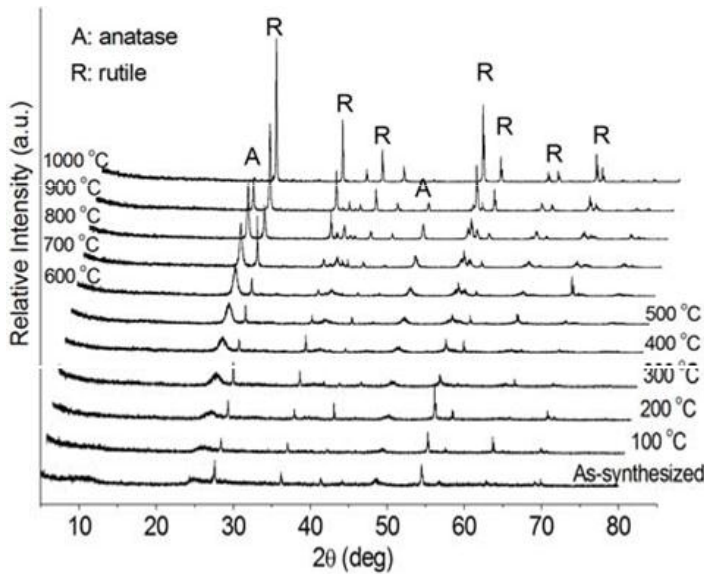


**Fig. 2** XRD patterns of the prepared sample calcined at various temperatures

**3.3 TEM of Ag – N Co-doped TiO<sub>2</sub> Nanocomposite**

TEM images of different Ag loaded N-doped TiO<sub>2</sub> nanocomposites are shown in Fig. 3. The size of the particles is in the range 10–15 nm, with the average particle size from representative TEM images to be around 10 nm which is in good agreement with the results obtained from XRD. As the Ag loading increased from 0.1 to 0.5 M, the particle size of as-synthesized nanomaterials were decreased and with further increase in Ag loading the particle size increased most likely as a result of agglomeration as seen in the TEM images.

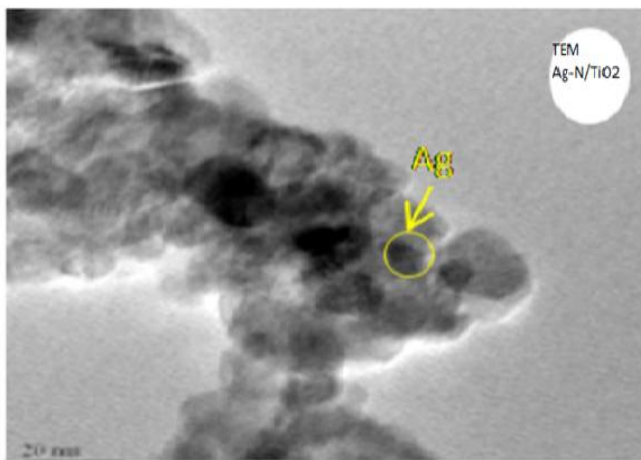


**Fig. 3** TEM image of Ag-N co-doped TiO<sub>2</sub>

**3.4 UV/Vis Absorbance Study**

Fig. 4 exhibits UV-Vis spectrum of Ag loaded N-doped TiO<sub>2</sub>. The absorption of Ag loaded N-doped TiO<sub>2</sub> exhibits a red shift, that is to say, the co-doped widens the light absorption range of TiO<sub>2</sub> from 395 nm to 540 nm and prolong the recombination time. Using (Equation 2) it is possible to estimate the band gap energy of ANT.

$$E_g(\text{eV}) = \frac{1240}{\lambda} \quad (2)$$

Where E<sub>g</sub> is band gap in electron volts, and λ is wave length at the intercept of the tangent line to the X- axis. Therefore λ of ANT was 540 nm and its band gap energy using (Equation 2) has been estimated to be 2.296 eV. From this measurement, the absorption edge of Ag-N co-doped TiO<sub>2</sub> shifts to visible light compared to non-doped TiO<sub>2</sub> with a maximum absorption band at 540 nm. This may be due to band gap narrowing of TiO<sub>2</sub> up on doping N, and inhibits the recombination time by Ag.

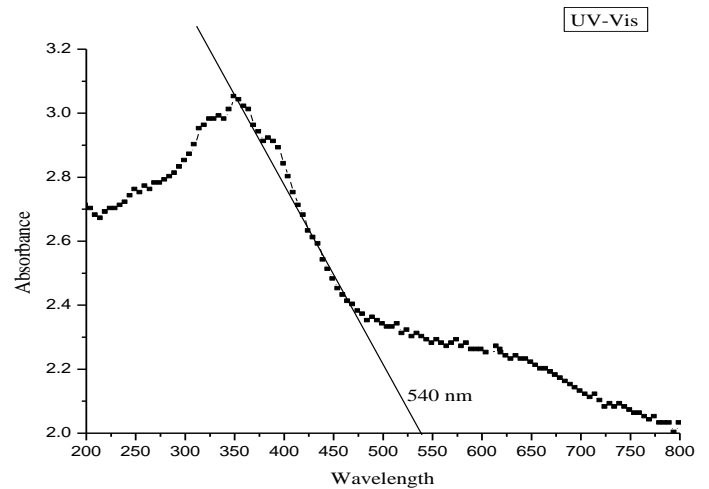


**Figure.4** UV/Vis absorbance edge of ANT

**3.5 Photocatalytic Degradation Process of Methyl orange**

In order to investigate the photocatalytic activity of the as-synthesized nanomaterial, photocatalytic degradation of methyl orange was carried out under UV and Visible radiations. The UV and visible light sources were kept at a distance of 9.00 cm from the solution and have 8.25mW per cm<sup>2</sup> intensity. The percentage degradation of MO at different time was calculated using (Equation 3)

$$\% \text{ Degradation} = \frac{(A_0 - A_t)}{A_0} \times 100\% \quad (3)$$

Where A<sub>0</sub> is the initial absorbance of reference MO solution and A<sub>t</sub> is the revised absorption considering MO after photo irradiation. The percentage degradation of MO in aqueous solution with out as-synthesized nanomaterial (blank) at 180 minutes under UV and Visible radiation was 0.91% and 3.05 respectively (Fig. 5&6).

**3.6 The effect of silver doping on Photocatalytic efficiency**

Fig. 5&6 present the photocatalytic decomposition of Ag-N/TiO<sub>2</sub> in different concentrations of silver. The results show that 50.34%, 74.56%, 78.23%, 87.42%, 55.35%, and 35.56% of the MO has been degraded using 0.1 M, 0.2018 M, 0.25 M, 0.5 M, 0.75 M and 1 M (Fig. 5) under visible irradiation. Similarly under UV irradiation 48.11%, 72.55%, 76.23%, 84.32%, 53.43%, 32.11% of the MO has been degraded (Fig. 6). Therefore, modification of N-doped TiO<sub>2</sub> by silver deposition increased amount of adsorbed MO in Ag-N/TiO<sub>2</sub> samples and then accelerated the process of MO

decomposition. The highest adsorption ability towards MO has been shown by 0.5 M, which also showed the highest MO decomposition under both UV and visible irradiation. For explain of this results, silver and TiO<sub>2</sub> have different work functions, ( $\Phi$  TiO<sub>2</sub> = 4.2 eV and  $\Phi$ Ag = 4.6 eV) [14]. So when silver contacts with N/TiO<sub>2</sub>, electrons will transfer from TiO<sub>2</sub> to silver. Those electrons transferred to silver and loaded on the surface of silver will be scavenged by the electron acceptor, thus decreases the recombination between electron and hole. Therefore, the existence of silver atom in Ag-N/ TiO<sub>2</sub> sheet can help more holes to transport to the surface and enhance the photocatalytic efficiency [14]. However, too much silver loading will result in a negative effect and photocatalytic degradation of MO decreases (Fig. 5&6). The main reason for the low efficiency are excessive coverage of TiO<sub>2</sub> catalyst limits the amount of light reaching to the TiO<sub>2</sub> surface, reducing the number of photogenerated e<sup>-</sup> - h<sup>+</sup> pairs and lowering consequently the TiO<sub>2</sub> photoactivity [15]. Fig. 5 shows that Ag-N/TiO<sub>2</sub>- visible photocatalysts achieved the highest photodegradation efficiency with a MO conversion of 87.42% after 180 minute of visible irradiation, followed by sample Ag-N/TiO<sub>2</sub>-UV (84.32%). This might be due to the strong adsorption capacity contributes greatly to the photodegradation for MO under visible light irradiation. Secondly, the Ag- N facilitate the spectral absorption in visible range which benefits for the harvest of visible light and consequently the improvement of photocatalytic activity of photocatalysts. Thirdly, Ag modification may cause the transferring of electrons from TiO<sub>2</sub> to the vicinity of Ag to form Schottky barriers, which improves the charge separation.

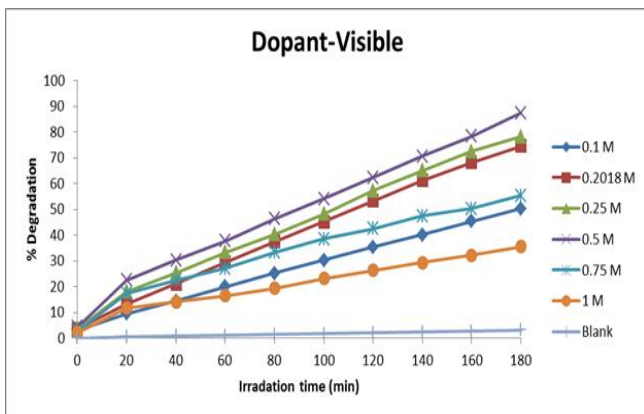


Figure 5. Effect of Ag concentration under visible light.

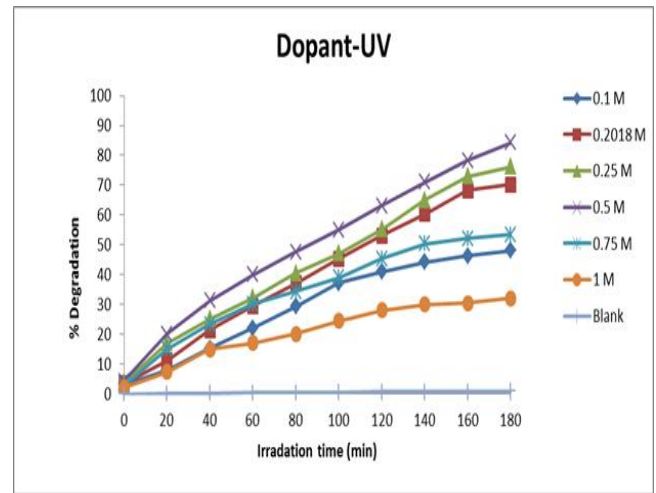
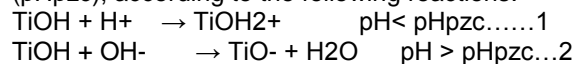


Figure 6. Effect of Ag concentration under UV irradiation.

### 3.7 Effect of pH on photocatalytic degradation of MO

The effects of pH on the photodegradation efficiency, which include optimum amount of Ag-N/TiO<sub>2</sub> (500 mg) photocatalyst and fixed concentration of MO (100 ppm) were examined in the pH range of 2-9. Fig. 7 and 8 indicated that the pH change does not show significant effect in the degradation of MO in the absence of Ag-N/TiO<sub>2</sub>, but gradually increase in the presence of Ag-N/TiO<sub>2</sub>. It could be noticed that the best result were obtained in acidic solution 88.33% (pH = 2), 74.55% (pH = 3) and 55.47% (pH = 4), after 3 hours under visible irradiation (Figure 8). Similarly, under UV irradiation was 84.55%, 72.14%, 52.18%, 41.75%, 20.03% and 13.48% of MO has been degraded at similar pH (Figure 9). Results indicate that the difference between the degree of disappearance of MO in strong acidic solution (pH = 2-3) and almost neutral (pH ≥ 6) was very important. The possible explanation for this result is the amphoteric behavior of semiconducting titanium dioxide and the change of surface charge properties of TiO<sub>2</sub> with the change pH values [16] around its point of zero charge (pH<sub>pzc</sub>), according to the following reactions.



Photocatalyst surface is positively charged in acidic media, whereas it is negatively charged under alkaline condition. Therefore, pH changes can thus influence the adsorption of MO molecule on to the TiO<sub>2</sub> surface, an important step for the photo-oxidation to take place. Further decrease in pH affected the photocatalytic activity of the catalyst negatively. Hence, the optimum pH for that particular catalysts' preparation was 2.0. The reason advanced for the adverse effect of low pH on the photocatalyst performance is that the possible increase of H<sup>+</sup> concentration may restrain hydrolyzation of the catalyst and the dye MO there by reduces the crystal size of the prepared Ag-N/ TiO<sub>2</sub> nanoparticles. Again, too low pH would result in phase transformation from anatase to rutile [17]. In alkaline solution, the MO molecules are negatively charged and their adsorption is also expected to be affected by an increase in the density of TiO<sup>-</sup> groups on the semiconductor surface. Thus, due to columbic repulsion, substrate is scarcely adsorbed [18]. At high pH values the hydroxyl radicals are so rapidly scavenged that they do not have the opportunity to react with dyes [19]. For the above reasons the photocatalytic activity of anionic dyes (mainly sulphonated dyes like MO)

reached a maximum in acidic conditions followed by a decrease in the pH range 7-11.

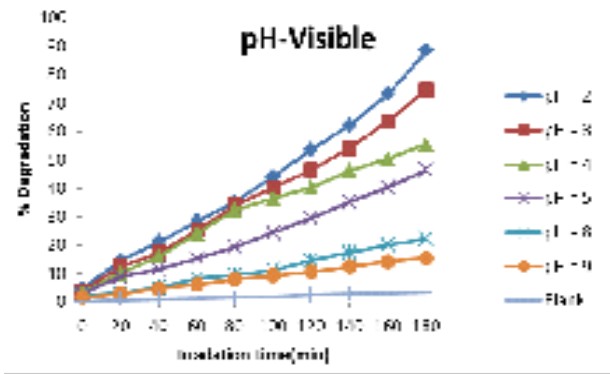


Figure 7. pH effect on the photodegradation of MO under visible irradiation

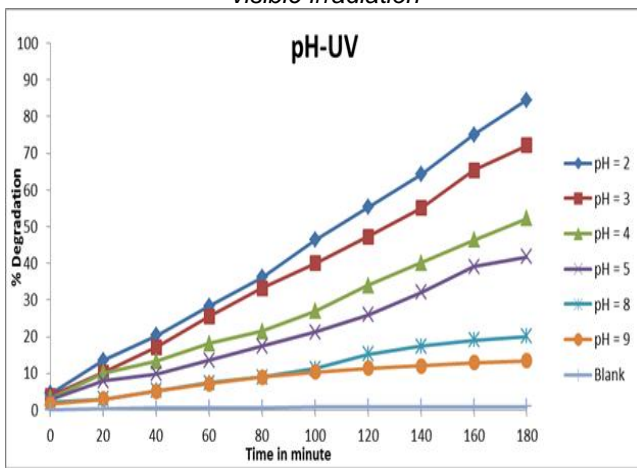


Figure 8. pH effects on the photodegradation of MO under UV irradiation.

### 3.8 Effect of catalyst loading

The effect of catalyst loading on photocatalytic degradation of MO under both visible and UV irradiation was studied using various amount of catalyst, from 200 mg/L to 700 mg/L by keeping other parameters identical. The effect of catalyst loading on photocatalytic degradation of MO is shown in (Fig. 9 & 10). A maximum 89.1 % and 78 % degradation of MO was obtained at 400 mg/L catalyst loading under visible and UV irradiation within 180 min respectively. Lastly as the concentration of the catalyst increases above the optimum value, the percentage degradation decreases. This may be due to the 'shielding effect' caused by the suspended TiO<sub>2</sub> layers located closer to the radiation source, which reduce the penetration of light.

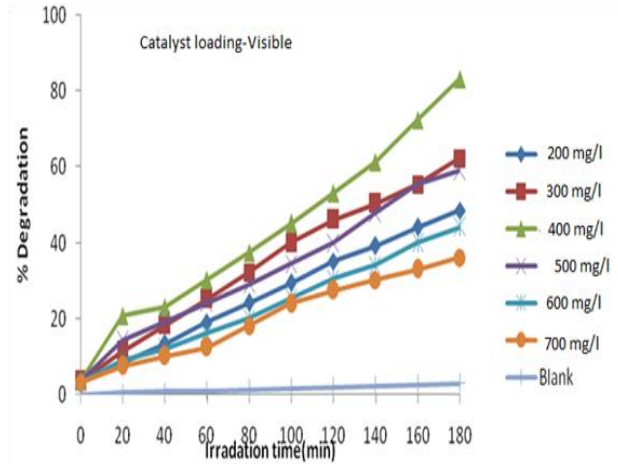


Figure 9. Effect of catalyst loading for photocatalytic degradation of MO under visible light

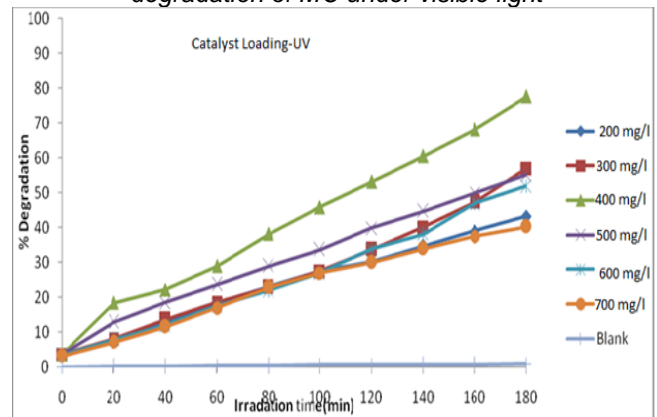


Figure 10. Effect of catalyst loading for photocatalytic degradation of MO under UV irradiation.

### 4. CONCLUSIONS

In this piece of work, it was found that the efficiency of the photocatalyst depends on the working conditions such as dopant concentration, calcination temperature, pH and catalyst loading of solution. The photocatalytic activity of Ag- N/TiO<sub>2</sub> was tested by photocatalytic degradation of methyl orange (MO) as a model compound of the textile dyes. Results show silver content has an optimum value of 0.5 M for achieving high photocatalytic activity. This is due to the presence of Ag on the surface of N/TiO<sub>2</sub> caused retarding the recombination reaction which occurs after excitation of semiconductor with UV and visible light. In good agreement with pH dependence of the photocatalytic degradation of MO, a strong adsorption was observed at pH values between 2 and 9 with a best result at pH = 2. This adsorption appeared to be an important parameter controlling the photodegradability of MO. The crystalline phase and morphology of the composite is depending on the calcination temperature. The titanate phase transformed to anatase at calcination temperature higher than 5000c. When the calcination temperature reached 10000c, only rutile phase was found in the XRD pattern. Therefore, optimization of the reaction conditions such as calcination temperature, catalyst loading, pH and dopant concentrations used to solve the issue of aggregation and to systematically

enhance the photocatalytic activity of Ag-N/TiO<sub>2</sub> under UV and visible light.

## ACKNOWLEDGEMENT

Nothing is impossible in the presence of the almighty God that makes me pass all the obstacles I Faced here and there. Thus, my solely priceless gratitude goes to the forever father God in heaven who gives me favor and mercy the whole time my stay in this college. Lastly, but not least, I thank Chemistry Department of Haramaya University for hosting me to pursue my M.Sc, as well as MOE and Korem wereda education office, for providing the financial assistance.

## REFERENCES

- [1] Bei Cheng, Yao Le, Jiaguo Yu Preparation and enhanced photocatalytic activity of Ag@TiO<sub>2</sub> core-shell nanocomposite nanowires *Journal of Hazardous Materials* 177 (2010) 971–977
- [2] Jiu-Hua Deng, Xiu-Rong Zhang, Guang-Ming Zeng, Ji-Lai Gong, Qiu-Ya Niu, Jie Liangus. Simultaneous removal of Cd(II) and ionic dyes from aqueous solution using magnetic graphene oxide nanocomposite as an adsorbent. *Chemical Engineering Journal* 226 (2013) 189–200
- [3] Alex Omo Ibadon and Paul Heterogeneous Photocatalysis: Recent Advances and Applications Fitzpatrick, *Catalysts* 2013, 3, 189-218
- [4] GUPTA Shipra Mital & TRIPATHI Manoj A review of TiO<sub>2</sub> nanoparticles, *Chinese Sci Bull* June 2011 Vol.56 No.16: 1639–1657
- [5] Ahmed A.Abd El-Rady, Mahmmoud S. Abd El-Sadek, Mohamed M. El-Sayed Breky<sup>1</sup>, Fawzy H. Assaf. Characterization and Photocatalytic Efficiency of Palladium Doped-TiO<sub>2</sub> Nanoparticles. *Advances in Nanoparticles*, 2013, 2, 372-377
- [6] Bei Cheng, Yao Le, Jiaguo Yu Preparation and enhanced photocatalytic activity of Ag@TiO<sub>2</sub> core-shell nanocomposite nanowires *Journal of Hazardous Materials* 177 (2010) 971–977
- [7] E. Pipelzadeh<sup>1</sup>, M. Valizadeh Derakhshan, A. A. Babaluo, M. Haghighi A. Tavakoli. Formic Acid Decomposition Using Synthesized Ag/TiO<sub>2</sub> Nanocomposite in Ethanol-Water Media Under Illumination of Near UV Light. *Int. J. Nanosci. Nanotechnol.*, Vol. 7, No. 2, Jun. 2011, pp. 78-86
- [8] A. Masoumi, M. Ghaemy. Adsorption of heavy metal ions and azo dyes by crosslinked nano-chelating resins based on poly(methylmethacrylate-co-maleic anhydride), *EXPRESS Polymer Letters* Vol.8, No.3 (2014) 187–196.
- [9] Lv, J., W. Gong, K. Huang, J. Zhu, F. Meng, X. Song and Z. Sun, 2011. Effect of annealing temperature on photocatalytic activity of ZnO thin films prepared by sol-gel method. *Superlattices and Microstructures*, 50(2): 98-106.
- [10] Zhaoyue Liu, Xintong Zhang, Shunsuke Nishimoto, Ming Jin, Donald A. Tryk, Taketoshi Murakami, and Akira Fujishima Langmuir, 2007. Anatase TiO<sub>2</sub> Nanoparticles on Rutile TiO<sub>2</sub> Nanorods. A Heterogeneous Nanostructure via Layer-by-Layer Assembly, 23(22):10916-10919.
- [11] Li, Y., S. Peng, F. Jiang, G. Lu, and S. Li, 2007. Effect of doping TiO<sub>2</sub> with alkaline-earth metal ions on its photocatalytic activity. *J. Serb. Chem. Soc*, 72 (4):393–402.
- [12] Chan, C.K., J.F. Porter, Y.G. Li, W. Guo, C.M. Chan, 1999. Photoactivity of anatase-rutile TiO<sub>2</sub> nanocrystalline mixtures obtained by heat treatment of homogeneously precipitated anatase. *J. Am. Ceram. Soc*, 82:566.
- [13] Parker, J.C., R.W. Siegel, 1990. Photoactivity of anatase-rutile TiO<sub>2</sub> nanocrystalline mixtures obtained by heat treatment of homogeneously precipitated anatase. *J. Mater. Res*, 5: 1246.
- [14] Tan, T.T.Y., C.K. Yip, D. Beydoun, R. Amal, 2003. Effects of nano-Ag particles loading on TiO<sub>2</sub> photocatalytic reduction of selenate ions. *Chem. Eng. J*, 95: 179–186.
- [15] Carp, O., C.L. Huisman, and A. Reller, 2004 Photoinduced reactivity of titanium oxide photoinduced reactivity of titanium oxide. *Solid State Chem*, 32 :33–177.
- [16] Marci, G., V. Augugliaro, A. Binaco, C. Biondi, E. Garcia-Lopez, V. Loddo, L. Palmisano, E. Pramauro and M. Schiavello, 2003. *Annali di Chimica* by Societa Chimica Italia, 93: 639-645
- [17] Chen, X and G. Gu, 2002. Study on synthesis of nanometer TiO<sub>2</sub> crystal from organic compound in liquid phase at normal pressure and low temperature. *J. Inorg. Chem*, 18 (7):749–752
- [18] Lachheb, H., E. Puzenal; A. Houas, M. Ksibi, E. Elaloui, C. Guillard and J.M. Herrmann, 2002. photocatalytic degradation of various types of dyes in water by UV-irradiation titania. *Applied Catalysis B. Environmental*, 39:75-90.
- [19] Tang, W.Z., Z. Zhang, H. An, M.O. Quintana and D.F. Torres, 1997. TiO<sub>2</sub>/UV photodegradation of azo dyes in aqueous solutions. *Environmental Technology*, 18:1-12.